Published in final edited form as:
Nat Immunol. ; 13(8): 753–760. doi:10.1038/ni.2360.

IL-34 is a tissue-restricted ligand of CSF1R required for the development of Langerhans cells and microglia

Yaming Wang[1], **Kristy J. Szretter**[1,2,3], **William Vermi**[1,4], **Susan Gilfillan**[1], **Cristina Rossini**[4], **Marina Cella**[1], **Alexander D. Barrow**[1,5], **Michael S. Diamond**[1,2,3], and **Marco Colonna**[1]

[1]Department of Pathology and Immunology, Washington University School of Medicine, St. Louis, Missouri, USA

[2]Department of Medicine, Washington University School of Medicine, St. Louis, Missouri, USA

[3]Department of Molecular Microbiology, Washington University School of Medicine, St. Louis, Missouri, USA

[4]Department of Pathology, University of Brescia, Brescia, Italy

[5]Department of Pathology, University of Cambridge, Cambridge, UK

Abstract

The differentiation of bone marrow–derived progenitors into monocytes, tissue macrophages and some dendritic cell (DC) subtypes requires the growth factor CSF1 and its receptor, CSF1R. Langerhans cells (LCs) and microglia develop from embryonic myeloid precursors that populate the epidermis and central nervous system (CNS) before birth. Notably, LCs and microglia are present in CSF1-deficient mice but absent from CSF1R-deficient mice. Here we investigated whether an alternative CSF1R ligand, interleukin 34 (IL-34), is responsible for this discrepancy. Through the use of IL-34-deficient (*Il34*$^{LacZ/LacZ}$) reporter mice, we found that keratinocytes and neurons were the main sources of IL-34. *Il34*$^{LacZ/LacZ}$ mice selectively lacked LCs and microglia and responded poorly to skin antigens and viral infection of the CNS. Thus, IL-34 specifically directs differentiation of myeloid cells in the skin epidermis and CNS.

INTRUCTION

The mononuclear phagocyte system encompasses a group of myeloid cells with crucial functions in maintaining the homeostasis of multiple tissues as well as promoting inflammatory and repair responses to microbial, chemical and physical insults[1–5]. The development of many mononuclear phagocytes, including blood monocytes and tissue macrophages, requires colony-stimulating factor 1 (CSF1; also known as macrophage colony-stimulating factor (M-CSF)[6,7]. CSF1 binds to and activates the tyrosine kinase receptor CSF1R (also known as M-CSFR or CD115) on bone marrow progenitors, which results in their proliferation and differentiation into monocytes and macrophages. The CSF-1–CSF1R ligand-receptor pair also promotes the differentiation of multinucleated osteoclasts[8], which are created by the fusion of mononuclear myeloid progenitors and

Correspondence should be addressed to: M.C. (mcolonna@pathology.wustl.edu).

AUTHOR CONTRIBUTIONS

Y.W., K.J.S. and M.Ce. designed, did and analyzed experiments and wrote the manuscript; W.V. and C.R. did immunohistochemical analysis; M.S.D. supervised CNS-infection experiments; S.G. and A.D.B. generated *Il34*$^{LacZ/LacZ}$ mice; and M.Co. supervised research and wrote the manuscript.

COMPETING FINANCIAL INTERESTS

The authors declare no competing financial interests.

participate in the resorption and remodeling of bone. Moreover, signaling via CSF1R contributes to the development of two dendritic cell (DC) subsets: Langerhans cells (LCs), which are the resident DCs of the epidermis; and monocyte-derived DCs, which constitute a major DC population in inflamed tissues[1–5,9].

Although monocytes, tissue macrophages, osteoclasts, monocyte-derived DCs and LCs express CSF1R, their dependence on CSF1 varies considerably[10]. This heterogeneity is reflected in the disparate phenotypes of osteopetrotic mutant mice that lack CSF1 because of an inactivating mutation (op/op) in the gene encoding CSF1 (*Csf1*$^{op/op}$ mice)[11] and mice deficient in CSF1R (*Csf1r*$^{-/-}$ mice)[12]. Both *Csf1*$^{op/op}$ and *Csf1r*$^{-/-}$ mice lack osteoclasts and thus are osteopetrotic. However, *Csf1r*$^{-/-}$ mice have more severe defects in several mononuclear phagocyte subsets than are *Csf1*$^{op/op}$ mice. Notably, microglia, which are the resident macrophages of the central nervous system (CNS)[13], are present in *Csf1*$^{op/op}$ mice but absent from *Csf1r*$^{-/-}$ mice[14,15]. Similarly, LCs are present in *Csf1*$^{op/op}$ mice but absent from *Csf1r*$^{-/-}$ mice[14,16]. Such discrepancies suggest the existence of an alternative ligand for CSF1R that can partially compensate for the absence of CSF1 in *Csf1*$^{op/op}$ mice. Relevant to this, interleukin 34 (IL-34) has been identified as the second functional ligand for CSF1R[17,18]. IL-34 shares little aminoacid homology with CSF1 but can bind to and activate CSF1R, at least *in vitro*[19,20]. Furthermore, transgenic expression of IL-34 'rescues' the bone, osteoclast and tissue macrophage defects of *Csf1*$^{op/op}$ mice[19]. Although IL-34 can compensate for the lack of CSF1, the expression patterns of *Il34* mRNA and *Csf1* mRNA are spatially and temporally distinct[19], which suggests that they have complementary rather than redundant roles in CSF1R activation *in vivo*.

In this study, we generated IL-34-deficient reporter mice in which the *Il34* coding sequence was replaced by the gene encoding β-galactosidase (*Il34*$^{LacZ/LacZ}$ mice). Analysis of these mice showed that IL-34 was produced mainly by keratinocytes and neurons. Consistent with that distribution pattern, we found that *Il34*$^{LacZ/LacZ}$ mice had a selective defect in the generation of LCs and microglia. The lack of LCs resulted in diminished contact hypersensitivity (CHS), whereas the deficiency in microglia resulted in greater susceptibility to viral infection of the CNS. In contrast to its effect on LCs and microglia, targeted deletion of *Il34* had little effect on other myeloid-cell compartments, except for slightly fewer CD11b^{+} DCs in the lung. Blood monocytes, other tissue macrophages and DC subsets were largely unaffected, reflective of the predominant role of other growth factors, such as CSF1 and Flt3, for their maturation.

LCs and microglia are unique among myeloid cells in their development; they arise from embryonic myeloid progenitors that populate the skin and the CNS, respectively, before birth. LCs and microglia proliferate before birth and during the first days of postnatal life and then self-renew with a slow turnover rate[13,16,21–23]. Our results show that IL-34 promotes a tissue-specific differentiation pathway that is selectively required for myeloid cells that populate the epidermis and CNS.

RESULTS

IL-34 expression mainly in the skin and CNS

We generated IL-34-mutant mice from a genetically targeted embryonic stem cell line designed to create a null, *lacZ* reporter allele by Cre-mediated deletion (Supplementary Fig. 1). We bred mice carrying the targeted *Il34* gene to transgenic mice expressing Cre driven bya ubiquitous cytomegalovirus promoter (CMV-Cre) to produce *Il34*$^{LacZ/+}$ mice in which exons 3–5 were deleted and replaced by an internal ribosome entry site–*lacZ* cassette. We intercrossed offspring to generate homozygous *Il34*$^{LacZ/LacZ}$ mice. To identify β-galactosidase (LacZ)-producing cells, we stained frozen tissue sections of *Il34*$^{LacZ/+}$ mice

with the β-galactosidase substrate X-gal. We found strong and punctate X-gal staining in the skin, brain, kidney and testes (Fig. 1). At the cellular level, X-gal staining was evident in keratinocytes, hair follicles, neurons, proximal renal tubule cells and seminiferous tubule germ cells. In the brain, we detected X-gal staining in the cerebral cortex and hippocampus but not in the cerebellum (Supplementary Fig. 2a–d). We did not find X-gal staining in the meninges, but it was present in a fraction of ependymal cells lining the ventricular system and those of the choroid plexus (Supplementary Fig. 2a–d), which suggested that IL-34 was secreted into the cerebrospinal fluid. X-gal staining was weak or undetectable in other nonlymphoid organs as well as spleen and lymph nodes (Fig. 1 and data not shown). X-gal staining in the CNS and skin substantially overlapped the pattern of *Il34* mRNA expression in the Biology Gene Portal System (BioGPS) microarray data set (http://biogps.org/#goto=genereport&id=76527) and its expression reported before[19]. In contrast, X-gal staining did not overlap the pattern of *Csf1* mRNA expression (http://biogps.org/#goto=genereport&id=12977), except in bones. These data indicated a nonredundant function for IL-34 in the CNS and skin, but a possibly redundant or dispensable role for IL-34 in other tissues in which CSF-1 is produced. *Il34* mRNA was almost undetectable in skin and brain of homozygous *Il34*$^{LacZ/LacZ}$ mice (Supplementary Fig. 2e, f), which confirmed that *Il34*$^{LacZ/LacZ}$ mice completely lacked IL-34.

IL-34 deficiency impairs epidermal LCs

Because we found that keratinocytes produced IL-34 (Fig. 1a), and LC development depends on CSF1R but not CSF1 (ref. 16), we hypothesized that IL-34 may be essential for the development of LCs. To test our hypothesis, we isolated cells from the ears of wild-type and *Il34*$^{LacZ/LacZ}$ mice and analyzed their content of LCs and dermal DCs by flow cytometry. We identified LCs as CD11c^{+} major histocompatibility complex class II (MHCII)$^{+}$ cells that express CD207 (langerin) but not CD103, which is a marker of some dermal DCs[2–4,22]. We categorized dermal DCs into two subsets. A larger subset included CD11c^{+}MHCII^{+} cells that lacked CD103 and CD207 (refs. 2–4,22). These cells also expressed the common myeloid marker CD11b (data not shown). A smaller subset included CD11c^{+}MHCII^{+} cells that expressed both CD103 and CD207 (refs. 24–28). We found considerably fewer CD11c^{+} MHCII^{+} CD103$^{−}$ CD207^{+} LCs in the skin of *Il34*$^{LacZ/LacZ}$ mice than in the skin of wild-type mice (Fig. 2a, b). In contrast, CD103^{+}CD207^{+} and CD103$^{−}$ CD207$^{−}$dermal DCs were equally abundant in *Il34*$^{LacZ/LacZ}$ and wild-type mice (Fig. 2a, b).

To confirm the defect in LCs and the maintenance of dermal DCs in the skin of *Il34*$^{LacZ/LacZ}$ mice, we isolated epidermal sheets from the ears of wild-type and *Il34*$^{LacZ/LacZ}$ mice and looked for LCs identified as CD11c^{+} and MHCII^{+} cells. The epidermis of *Il34*$^{LacZ/LacZ}$ mice had considerably fewer CD11c^{+}MHCII^{+} cells than did the epidermis of wild-type mice, as shown by both confocal microscopy (Supplementary Fig. 3a, b) and flow cytometry (Supplementary Fig. 3c, d). We also examined dermal DCs, identified as CD11c^{+}MHCII^{+} cells in the dermal sheets of the ears. Wild-type and *Il34*$^{LacZ/LacZ}$ mice had a similar frequency of dermal CD11c^{+}MHCII^{+} cells (Supplementary Fig. 3e, f). Dermal DC subsets, identified as CD103$^{−}$CD11b^{+} and CD103^{+}CD11b$^{−}$ cells, were present in equal abundance in wild-type and *Il34*$^{LacZ/LacZ}$ mice (Supplementary Fig. 3g–j). We also evaluated LCs and dermal DCs in the body-wall skin by assessing the expression of CD207, MHCII and CD11b by immunohistochemistry. *Il34*$^{LacZ/LacZ}$ mice had almost no cells that expressed CD207, MHCII and CD11b in the epidermis, whereas these cells were present in the dermis (Fig. 2c–e). Wild-type mice had cells that expressed CD207, MHCII and CD11b in both the epidermis and dermis.

Because LCs migrate from the skin to the lymph nodes[4,22], we analyzed skin-draining lymph nodes by flow cytometry. To distinguish among DC subsets, we costained lymph

node cells for CD11c and MHCII (Fig. 2f–h). $CD11c^{+}MHCII^{hi}$ cells (gate I) include migrating DCs; $CD11c^{+}MHCII^{int}$ cells (gate II) include $CD8\alpha^{+}$ DCs; $CD11c^{+}MHCII^{lo}$ cells (gate III) include plasmacytoid DCs. To further distinguish between LCs and dermal DCs, we also stained cells for CD103 and CD207, as described above. We noted considerably fewer migrating $CD103^{-}CD207^{+}$ LCs in *Il34*$^{LacZ/LacZ}$ mice than in wild-type mice (Fig. 2f–h). In contrast, migrating dermal DCs, including $CD103^{+}CD207^{+}$ and $CD103^{-}CD207^{-}CD11b^{+}$ subsets, were present in equal abundance in the lymph nodes of *Il34*$^{LacZ/LacZ}$ and wild-type mice (Fig. 2f–h). IL-34 deficiency had no effect on lymph node $CD8\alpha^{+}$ DCs or Siglec-H^{+} plasmacytoid DCs (Fig. 2f). Immunohistochemical analysis of lymph nodes showed considerably fewer CD207 cells in *Il34*$^{LacZ/LacZ}$ mice than in wild-type mice (Fig. 2i). Although some dermal DCs also express CD207 (refs. 24–28), the flow cytometry analysis indicated that the lower abundance of $CD207^{+}$ cells in the lymph nodes solely reflected a lower abundance of migrating epidermal LCs. Moreover, *Il34*$^{LacZ/LacZ}$ mice and wild-type mice had similar numbers of $CD207^{+}$ cells in the spleen and thymus (Supplementary Fig. 3k), consistent with the idea that these cells are not derived from epidermal LCs[24,25].

IL-34 deficiency affects T cell priming in CHS

LCs are antigen-presenting cells of the epidermis[29] that prime T cell responses to skin allergens[30–33]. Given that, we assessed the effect of IL-34 and LC deficiency on CHS. We sensitized wild-type and *Il34*$^{LacZ/LacZ}$ mice to the hapten DNFB by cutaneous application of DNFB to the shaved abdomen on day 0. After 5 d, we challenged mice by painting the left ear with DNFB and the right ear with vehicle only, as a control. We calculated ear swelling for each mouse by subtracting the thickness of the vehicle-treated ear from that of the DNFB-treated ear. Ear swelling in wild-type mice peaked between days 1 and 2 after challenge and decreased at day 3 (Fig. 3a). At all times after challenge, *Il34*$^{LacZ/LacZ}$ mice were less sensitive than were wild-type mice to DNFB-mediated CHS.

Because LCs deliver skin antigens to draining lymph nodes[34], we assessed whether the diminished CHS in *Il34*$^{LacZ/LacZ}$ mice depended on defective antigen delivery. We painted the ears of wild-type and *Il34*$^{LacZ/LacZ}$ mice with the dye CellTracker Green and monitored $CellTracker^{+}$ cells in the draining cervical lymph nodes 40–48 h later. To distinguish between skin-derived DCs and resident DCs, we costained lymph node cells for CD40 and CD11c[35]. The frequency of $CellTracker^{+}$ cells among $CD40^{hi}CD11c^{hi}$ DCs was much lower in *Il34*$^{LacZ/LacZ}$ mice than wild-type mice (Fig. 3b, population II), which suggested that $CD40^{hi}CD11c^{hi}$ DCs included migrating LCs. In contrast, the frequency of $CellTracker^{+}$ cells among $CD40^{int}CD11c^{int}$ cells was similar in the draining lymph nodes of wild-type and *Il34*$^{LacZ/LacZ}$ mice (Fig. 3b, population I), which suggested that the $CD40^{int}CD11c^{int}$ cells corresponded to migrating dermal DCs. Resident DCs, identified as $CD40^{lo}CD11c^{hi}$, were negative for CellTracker (Fig. 3b, population III) and were present in equal abundance in wild-type and *Il34*$^{LacZ/LacZ}$ mice. Thus, deficiency of IL-34 resulted in selectively fewer $CellTracker^{+}$ cells of epidermal origin in the draining lymph nodes. To confirm those results, we evaluated migrating LCs and dermal DCs in the lymph nodes after painting with CellTracker Green, using CD207 and CD103 as markers. The draining lymph nodes of *Il34*$^{LacZ/LacZ}$ mice had considerably fewer $CellTracker^{+}CD207^{+}CD103^{-}$ LCs than did those of wild-type mice, whereas we observed a similar proportion of $CellTracker^{+}CD207^{+}CD103^{+}$ dermal DCs in *Il34*$^{LacZ/LacZ}$ and wild-type mice (Fig. 3c).

$CD8^{+}$ and $CD4^{+}$ T cells that produce interferon-γ (IFN-γ) mediate CHS to DNFB[36]. Thus, we examined the effect of deficiency in IL-34 and LCs on the priming of T cells in draining lymph nodes after sensitization with DNFB. We collected inguinal lymph nodes 6 d after sensitizing mice with DNFB, then stimulated the lymph nodes with plate-bound antibody to

CD3 (anti-CD3) and assessed IFN-γ production 24 and 48 h later. Lymph node cells from *Il34*$^{LacZ/LacZ}$ mice produced less IFN-γ than did cells isolated from wild-type mice (Fig. 3d). Lower IFN-γ production was paralleled with fewer total cells in the lymph nodes of *Il34*$^{LacZ/LacZ}$ mice than in the lymph nodes of wild-type mice, consistent with the lower inflammation (Supplementary Fig. 4a). The lack of IL-34, however, had no effect on the normal development of $CD8^+$ or $CD4^+$ T cells in the thymus or the number of $CD8^+$ or $CD4^+$ T cells in lymph nodes of naive mice (Supplementary Fig. 4b). Together these results demonstrated that the paucity of epidermal LCs due to lack of IL-34 impaired antigen delivery and priming of allergen-specific T cells in local draining lymph nodes.

It has been shown that LCs are necessary and sufficient for direct antigen presentation and the generation of an antigen-specific response by the T_H17 subset of helper T cells in a model of infection of the skin with *Candida albicans*[37]. To see whether IL-34 and LC deficiency affected the skin response to *C. albicans*, we sensitized *Il34*$^{LacZ/LacZ}$ and wild-type mice by applying *C. albicans* to shaved dorsal skin. One week after sensitization, we challenged mice with *C. albicans* in the footpad and measured swelling the next day. *Il34*$^{LacZ/LacZ}$ mice had modestly but significantly ($P = 0.0237$) less swelling than did wild-type mice (Supplementary Fig. 4c). We found fewer cells in the draining lymph nodes of *Il34*$^{LacZ/LacZ}$ mice than in those of wild-type mice (Supplementary Fig. 4d), which provided further evidence of an attenuated inflammatory skin response to *C. albicans*. This result confirmed the CHS data and indicated that the lack of LCs did have at least some effect on delayed-type hypersensitivity responses to pathogens in the skin.

IL-34 deficiency impairs microglia cell numbers

Because we found that neurons produced IL-34 (Fig. 1b and Supplementary Fig. 2a, *c*) and microglia are present in *Csf1*$^{op/op}$ mice but absent from *Csf1r*$^{-/-}$ mice[14,15], we hypothesized that IL-34 contributes to the development of microglia. We purified myeloid cells from the brains of *Il34*$^{LacZ/LacZ}$ and wild-type mice with anti-CD11b magnetic beads and identified microglia ($CD11b^+CD45^{int}$) by flow cytometry[13]. The number of $CD11b^+CD45^{int}$ cells isolated from brains of *Il34*$^{LacZ/LacZ}$ mice was <20% of that in wild-type mice (Fig. 4a). Staining of CNS sections with IBA-1, a marker of myeloid cells, confirmed that the cerebral cortex, corpus callosum, hippocampus and basal ganglia of *Il34*$^{LacZ/LacZ}$ mice had considerably fewer microglia than did those of wild-type mice (Fig. 4b–e and Table 1). Notably, the cerebellum of *Il34*$^{LacZ/LacZ}$ mice and wild-type mice had a similar abundance of microglia (Fig. 4f and Table 1), perhaps because of local production of CSF1. We purified residual microglia of *Il34*$^{LacZ/LacZ}$ mice and stimulated them *in vitro* with ligands of Toll-like receptors (TLRs). Purified microglia from *Il34*$^{LacZ/LacZ}$ mice produced inflammatory cytokines in amounts similar to those produced by equal numbers of wild-type microglia (Supplementary Fig. 5a), which indicated that IL-34 deficiency affected mainly development but not the ability of microglia to produce inflammatory cytokines.

IL-34 deficiency affects antiviral resistance in the CNS

Microglia are thought to protect the CNS from viral infection through several mechanisms, including the production of cytokines that inhibit viral replication, the phagocytosis of virus-infected and dying neurons and the induction of neuronal repair and homeostasis[13]. We examined the effect of deficiency in IL-34 and microglia *in vivo* during infection with a neurotropic virus. We infected wild-type and *Il34*$^{LacZ/LacZ}$ mice with West Nile virus (WNV) via an intracranial route and monitored survival. Infection with wild-type virulent WNV resulted in rapid mortality in both *Il34*$^{LacZ/LacZ}$ mice and wild-type mice, as 100% of both groups of mice succumbed to infection by 8 d after infection (Fig. 5a). In contrast, when we infected mice with an attenuated WNV strain (WNV-E218A), we observed more death of *Il34*$^{LacZ/LacZ}$ mice than of wild-type mice by 10–12 d after infection. This result

suggested that a lack of IL-34 and consequent lower abundance of microglia impaired CNS defenses against WNV infection. Notably, we detected similar viral burdens in various regions of the brain of wild-type and *Il34*$^{LacZ/LacZ}$ mice on both day 3 and day 6 after infection (Supplementary Fig. 5b), which suggested that the protective effect of microglia may have been due to their ability to limit neuronal death and/or promote CNS repair rather than their ability to directly inhibit viral replication.

To test that hypothesis, we assessed neuronal apoptosis in various regions of the brains of wild-type and *Il34*$^{LacZ/LacZ}$ mice on day 6 after infection by TUNEL (terminal deoxynucleotidyl transferase-mediated dUTP nick end-labeling) assay. *Il34*$^{LacZ/LacZ}$ mice had more neuronal apoptosis in all brain areas analyzed (Fig. 5b–f). Analysis of WNV-infected brains by flow cytometry showed that *Il34*$^{LacZ/LacZ}$ mice had fewer microglia than did wild-type mice (Supplementary Fig. 5c). Thus, although WNV infection causes inflammation and the recruitment of bone marrow–derived myeloid cells, such as inflammatory monocytes[38], such recruitment was not sufficient to compensate for the defect in resident microglia in *Il34*$^{LacZ/LacZ}$ mice. WNV-infected *Il34*$^{LacZ/LacZ}$ and wild-type mice had a similar abundance of brain macrophages and total CD4$^+$ T cells and CD8$^+$ T cells, as well as WNV-specific CD8$^+$ T cells (Supplementary 5c–e), which further suggested that susceptibility of *Il34*$^{LacZ/LacZ}$ mice to WNV was due to insufficient resident microglia and a consequent lack of the protective and trophic factors provided by these cells.

Limited effect of IL-34 on other macrophage and DC subsets

In vitro studies have suggested that IL-34 can promote differentiation of bone marrow–derived macrophages (BMDMs)[19]. Furthermore, transgenic expression of IL-34 ‘rescues’ the bone, osteoclast and tissue macrophage defects of *Csf1*$^{op/op}$ mice[19]. Whether IL-34 is necessary for the development of macrophages *in vivo* in tissues other than the skin and the brain remains unknown. To assess this, we examined whether IL-34 deficiency affected myeloid cell development in lymphoid organs. Notably, *Il34*$^{LacZ/LacZ}$ and wild-type mice had similar frequencies of CD11b$^+$, F4/80$^+$, Ly6C$^+$ and Ly6G$^+$ cell subsets in the peripheral blood and bone marrow (Supplementary Fig. 6a). Analysis of DC subsets in the spleens of *Il34*$^{LacZ/LacZ}$ and wild-type mice also showed a similar frequency of CD8α$^+$, CD11b$^+$ and CD4$^+$CD11c$^+$ DCs as well as Siglec-H$^+$ plasmacytoid DCs (Supplementary Fig. 6b).

We next assessed whether IL-34 deficiency also affected the development of tissue-resident macrophages in nonlymphoid organs. Kupffer cells are liver-resident macrophages[39] that include two subsets identified by expression of the macrophage marker F4/80 and CD11b[40]. The frequency of F4/80$^+$CD11b$^-$ and F4/80$^+$CD11b$^+$ Kupffer cells was similar in *Il34*$^{LacZ/LacZ}$ and wild-type mice (Fig. 6a). IL-34 deficiency also had no effect on lung alveolar macrophages, identified as CD11c$^+$Siglec-F$^+$F4/80$^+$ cells (Fig. 6b), or total DCs, identified as CD11c$^+$Siglec-F$^-$ cells (Fig. 6c). However, among lung DC subsets, *Il34*$^{LacZ/LacZ}$ mice had fewer CD11c$^+$CD11b$^+$ DCs (Fig. 6b, c). These results suggested a smaller effect of IL-34 on the development of macrophages and DCs than on the development of LCs and microglia, probably because of redundancy with CSF-1.

The development of microglia and LCs require IL-34

Microglia and LCs originate during embryogenesis from primitive precursors that populate the skin and CNS before birth. Precursor cell populations expand before and soon after birth. In the adults, microglia and LCs self-renew with a slow turnover rate under homeostatic conditions[13,16,21–23]. We sought to determine whether the defects in LCs and microglia observed in adult *Il34*$^{LacZ/LacZ}$ mice was due to impaired development or maintenance in the adult once these cells developed. To address this, we examined microglia and LCs in neonates. *Il34*$^{LacZ/LacZ}$ neonates had considerably fewer microglia than did wild-type

neonates (Fig. 7a, b). Similarly, although they were present in wild-type neonates, LCs were absent from the skin of *Il34*$^{LacZ/LacZ}$ mice (Fig. 7c, d). Thus, IL-34 was crucial for the development of both cell subsets.

LC recovery after inflammation is IL-34 independent

We next assessed whether IL-34 was necessary for the turnover of LCs during skin inflammation. It has been shown that after prolonged exposure to ultraviolet light, LCs rapidly disappear and are replaced by circulating monocytic precursors within 3 weeks[41]. We depleted wild-type and *Il34*$^{LacZ/LacZ}$ mice of LCs by exposing them to ultraviolet light and analyzed the epidermis of the ears 21 d after treatment. In wild-type mice, after the initial depletion caused by exposure to ultraviolet light (Supplementary Fig. 7), LCs were partially replenished by day 21 (Fig. 7e, f). Notably, *Il34*$^{LacZ/LacZ}$ mice, which lacked LCs before the treatment with ultraviolet light, had a detectable LC population at day 21 (Fig. 7e, f), which suggested that IL-34 was dispensable for the regeneration of LCs from monocytic progenitors in adult mice in response to inflammation.

DISCUSSION

In this study, we showed that IL-34 was produced mainly by keratinocytes and neurons and that a lack of this cytokine resulted in considerably fewer LCs in the epidermis and microglia in the CNS. These results explain the well-described difference in the phenotypes of *Csf1*$^{op/op}$ mice and *Csf1r*$^{-/-}$ mice[12]: LCs and microglia are present in *Csf1*$^{op/op}$ mice but absent from *Csf1r*$^{-/-}$ mice[14–16]. Thus, IL-34 selectively directs a developmental program specific for these unique subsets of myeloid cells. Both LCs and microglia develop from embryonic progenitors and populate their correspondent tissues during embryogenesis. There, they proliferate and differentiate before and soon after birth[15,16,21]. We envision that IL-34 stimulates the population expansion and/or differentiation of the LC and microglia progenitors once they reach the epidermis and CNS. Consistent with such a model, we found that *Il34*$^{LacZ/LacZ}$ mice lacked LCs and microglia at birth. It is possible that IL-34 also contributes to the maintenance of LCs and microglia in the steady state in the adult. However, as *Csf1*$^{op/op}$ mice have LCs at birth[12] but are deficient in LCs as adults[42], CSF1 also may contribute to the self-renewal of LCs. Notably, we found IL-34 in ependymal cells of the choroid plexus, which suggests that it may promote the development of myeloid cells at this site, although DCs in the choroid plexus are dependent on the ligand for Flt3 (ref. 43).

After epidermal damage and inflammation, LCs are replaced rapidly by monocytic precursors[16]. Similarly, during CNS injury, bone marrow–derived progenitors infiltrate the CNS to promote inflammation and repair[38,44]. In these situations, the breakdown of the epidermis and altered brain-blood barrier probably facilitates the infiltration of bone marrow–derived myeloid progenitors and additional cellular sources of CSF1 that may contribute to the regeneration of LCs and microglia. In support of that model, we found that after ultraviolet light–induced inflammation, the defect of LCs in *Il34*$^{LacZ/LacZ}$ mice was partially compensated for by LCs presumably derived from monocytic precursors[41]. Although brain infection with an attenuated WNV virus did not lead to the complete replenishment of microglia by incoming monocytes, this may occur in mice infected with virulent strains that cause more severe inflammation.

In addition to finding IL-34 production in the epidermis and neurons, we detected IL-34 production in other tissue compartments, particularly the kidney and testis, but also in a scattered pattern in the spleen. Given those findings, it is likely that IL-34 also contributes to the development of myeloid cells in other anatomic regions. However, *Il34*$^{LacZ/LacZ}$ mice were fertile and lacked apparent renal deficiency. Moreover, *Il34*$^{LacZ/LacZ}$ mice had no apparent defects in blood monocytes, tissue macrophages or DCs, with the exception of

fewer $CD11c^+CD11b^+$ DCs in the lung. Thus, beyond the epidermis and CNS, cellular sources of CSF1 may compensate for an absence of IL-34. In some compartments, such as the skeletal system, CSF1 may act as the main agonist of CSF1R, as *Csf1*$^{op/op}$ mice develop osteopetrosis despite producing normal amounts of IL-34.

Because they selectively lacked LCs and microglia, *Il34*$^{LacZ/LacZ}$ mice provided a unique opportunity for assessing the function of these cells. LCs are antigen-presenting cells that intercalate with keratinocytes and establish tight contacts via E-cadherin-mediated adhesion[29,45]. Given the production of IL-34 by keratinocytes, such contacts may be essential for the differentiation and maintenance of LCs. LCs slowly detach from keratinocytes to cross the epidermal basement membrane and migrate into the draining lymph nodes and thus regulate skin-adaptive immune responses to physical injury, chemical allergens and infection[46]. Whether LCs elicit activation or tolerance of T cells in response to chemical allergens remains unclear[46]. One study has reported that mice with transgenic expression of the gene encoding diphtheria toxin under control of the human langerin promoter have constitutive deletion of LCs that results in enhanced CHS[47,48]. Thus, LCs seemed to have a tolerogenic function. However, conflicting results have been obtained with mice in which the gene encoding the receptor for diphtheria toxin is knocked into the langerin locus, so that LCs can be ablated conditionally by injection of diphtheria toxin. In these mice, deletion of LCs results in attenuated CHS[30,31] or has a negligible effect[34], which suggests that LCs have either a stimulatory function or no influence on T cell responses. CHS was attenuated in our *Il34*$^{LacZ/LacZ}$ mice relative to that in wild-type mice, which supports the proposal that LCs promote T cell stimulation, at least in response to a chemical hapten. The discrepancies among the studies may reflect differences in the extent and timing of LC defects as well as the type and amount of haptens and adjuvants used to induce CHS. Our study also showed that deficiency of IL-34 diminished the delayed-type hypersensitivity response to *C. albicans*, which supports the idea that LCs can promote the generation of T cell responses to pathogens[37].

It was unexpected that the considerably lower abundance of microglia in *Il34*$^{LacZ/LacZ}$ mice did not cause a substantially altered CNS phenotypes under steady-state conditions, although we did no detailed neurological testing. However, it is possible that loss of the neuroprotective functions of microglia may expedite neurodegenerative pathology[49]. Alternatively, microglia may have a role in synaptic pruning during postnatal development, which would influence brain plasticity[50]. Thus, it will be important in future studies to use IL-34-deficient mice to assess whether a lack of microglia induces functional changes in mouse behavior. The lack of microglia did negatively affect the survival of *Il34*$^{LacZ/LacZ}$ mice infected intracranially with an attenuated strain of WNV. However, microglia did not directly affect viral replication, as *Il34*$^{LacZ/LacZ}$ and wild-type mice had similar viral burdens in many brain regions, which suggests that in these settings, microglia may act by preserving CNS integrity, presumably by removing virus-infected, dying cells, secreting neurotrophic factors and limiting neuronal injury and death[13]. In summary, our studies of *Il34*$^{LacZ/LacZ}$ mice have demonstrated an alternative pathway for the development of myeloid cells that is essential for LCs and microglia but redundant or dispensable for other myeloid-cell subsets. Functional analysis of *Il34*$^{LacZ/LacZ}$ mice has defined an important role for LCs in promoting CHS and for microglia in protecting the CNS from injury associated with viral infection.

METHODS

Generation of *Il34*$^{LacZ/LacZ}$ mice

Of three clones carrying the targeted allele *Il34*$^{tm1a(EUCOMM)Wtsi}$ (European Conditional Mouse Mutagenesis Consortium), two were confirmed by Southern blot analysis as being

correctly targeted and were introduced into C57BL/6J-*Tyrc-2J*/J (B6-albino) eight-cell embryos by laser-assisted injection. Male chimeras (n = 18; most >80% derived from embryonic stem cells, as assessed by coat color) were obtained from clone EPD0146_4_D03 (embryonic stem line JM8.N4; C57BL/6). Chimeras were initially bred to B6-albino mice for analysis of germline transmission; those transmitting 100% were bred to CMV-Cre mice (>99% C57BL/6)[51] for deletion of exons 3–5 of *Il34* and the neomycin-resistance cassette; $Il34^{LacZ/+}$ offspring were intercrossed to generate IL-34-null $LacZ^{+}$ mice ($Il34^{LacZ/LacZ}$). To delete the IRES-lacZ–neomycin-resistance cassette and generate mice carrying a *lox*P-flanked *Il34* allele ($Il34^{f/+}$), chimeras were also bred to CAG-FLPe C57BL/6 transgenic mice[2], which express an enhanced form of the FLP recombinase driven by a chicken β-actin/rabbit β-globin hybrid promoter (AG) and the human CMV-IE enhancer. $Il34^{f/+}$ mice were intercrossed to generate $Il34^{f/f}$ mice (Supplementary Fig. 1). Homozygous $Il34^{LacZ/LacZ}$ mice were used for analysis; wild-type controls were age- and sex-matched C57BL/6 or $Il34^{f/f}$ mice bred in the same room of the facility. All animal studies were approved by the Washington University Animal Studies Committee. Mice were genotyped by PCR with the following oligonucleotides: for $Il34^{LacZ/LacZ}$, *Il34* 305959 (5′-TCAGATACAAATATGAAATTAGAG-3′), *Il34* 306329 (5′-TGCTGGCAAAGGGCTAAGAA-3′) and *Il34* 306539 (5′-GTCAGTATCGGCGGAATT-3′; wild-type product, 421 base pairs (bp); Editor: this PCR is deisigned to distinguish 3 possibilites: the endogenous allele, the external lox P site (5′ on our map, but not relevant otherwise) that is present in both the intitial targeted allele and in the floxed allele (post FLP), and the LacZ reporter (post Cre, exons 3–5 deleted) allele; have tried to make this more clear] *Il34* external LoxP product, 371 bp; *Il34*LacZ reporter product, 581 bp); for $Il34^{f/f}$, *Il34* 307868 (5′-CCATGGTCAGAGTCCCCAGG-3′) and *Il34* 315341 (5′-CCCTGGTCGGCTTTGCATGT-3′; wild-type product, 468 bp; *Il34*f product, 570 bp).

Immunohistochemistry and immunofluorescence

Sections for immunohistochemistry were obtained from formalin-fixed, paraffin-embedded tissues or frozen tissues. For morphology, slides were stained with hematoxylin and eosin. Cryostat sections 5 μm in thickness were air-dried overnight, fixed in acetone for 10 min and stained by with a β-Galactosidase Reporter Gene Staining Kit (Sigma). X-gal Stock Solution (Sigma) was prepared in *N*,*N*-dimethylformamide (Sigma). An X-gal working solution was prepared by dilution of the X-gal stock solution 1:40 in prewarmed dilution buffer. Slides were washed for 5 min at 25 °C in 1× PBS (Sigma) with three changes of the solution and were incubated for 4 h at 37 °C in X-gal working solution, in a humidified chamber. Sections were rinsed in 1× PBS (twice for 5 min each) and in distilled water (5 min). Sections were counterstained with hematoxylin or fast red. The β-galactosidase activity was visualized as a light blue signal. Sections (4 μm in thickness) from fixed tissues were stained with anti-IBA1 (rabbit; 1:300 dilution; Cat. No. 019-19741; Wako Chemicals) and reactivity was detected with an EnVision HRP-linked Rabbit kit (Dako) followed by diaminobenzidine. Nuclei were counterstained with haematoxylin. Cryostat sections (5 μm in thickness) from frozen tissues were stained with rat monoclonal antibody to langerin (1:100 dilution; 929F3.01; Dendritics), F4/80 (1:50 dilution; BM8; Caltag Laboratories), CD11b (1:100 dilution; M1/70; BD Pharmingen) or MHC class II I-A and I-E (1:50 dilution; 2G9; BD Pharmingen). Reactivity was detected with a Rat-on-mouse HRP-Polymer Kit (Biocare Medical) followed by diaminobenzidine as the chromogen. For microphotographs, immunostained sections were photographed with a DP-70 Olympus camera mounted on an Olympus BX60 microscope. Microglia in wild-type and mutant mice were quantified by staining with anti-IBA-1 (Cat. No. 019-19741; Wako Chemicals) in paired regions of the brain. At least 25 high-power-fields (magnification, ×400) per region were analyzed for each mouse with a Nikon Eclipse 50i. Freshly isolated epidermal sheets

were fixed and rehydrated and the receptor FcγR was blocked with monoclonal antibody 2.4G2 (ATCC). Epidermal sheets were stained with biotin-conjugated antibody to MHC class II (M5/114.15.2; BD Pharmingen) followed by streptavidin–Texas Red before being mounted on slides and analyzed with a Zeiss LSM 510 laser-scanning confocal microscope. At least eight high-power fields (magnification, ×400) per dermal sheet were analyzed. After infection with WNV, brains were collected and perfused sequentially with 20 ml PBS and 20 ml 4% paraformaldehyde in PBS, then fixed overnight at 4 °C in 4% paraformaldehyde in PBS. Tissues were cryoprotected in 30% sucrose and embedded, then frozen sections were cut. Tissues were prepared and stained as described[3]. After saturation of nonspecific binding sites and permeabilization of cells, sections were incubated overnight at 4 °C with anti-MAP2 (AP-20Chemicon). Primary antibodies were detected with secondary Alexa Fluor 488–conjugated goat anti-mouse IgG (Cat. No. A11017Molecular Probes). Nuclei were counterstained with To-Pro3 (Molecular Probes). TUNEL staining was done with an *in situ* cell death detection kit according to the manufacturer's instructions (Roche), with some modifications[53,54]. Fluorescence staining was visualized and quantified with a Zeiss 510 Meta LSM confocal microscope.

Quantitative PCR

RNA was extracted from skin and brain with an RNeasy Fibrous Tissue Mini kit as recommended by the manufacturer (Qiagen). After cDNA was synthesized from RNA with the Superscript III first-strand synthesis system for RT-PCR (Invitrogen), RNA expression was analyzed by quantitative PCR. SYBR Green PCR Master Mix (Bio-Rad Laboratories) and an ABI7000 (Applied Biosystems) were used according to the manufacturers' instructions. IL-34 expression was detected with oligonucleotides that specifically amplify a 171-bp fragment from cDNA encoding exon 6 (forward primer, 5′-TACAGCCACCTCTGCTTGTG-3′; reverse primer, 5′-GCAAGATACGGCATTTGGTT-3′).

Cell isolation

Epidermal sheets were separated by treatment of mouse ears for 1 h at 37 °C with Dispase I (Sigma) at a concentration of 2 U/ml. For single-cell suspensions, epidermis or dermis was minced into fine pieces and incubated for 1 h at 37 °C in collagenase IV (4830 U/ml; Sigma) and DNAse I (0.1 mg/ml; Sigma). Kupffer cells were isolated as described[55]. Livers were minced and then treated for 1 h at 37 °C with collagenase D (100 μg/ml, Sigma). Cells in single-cell suspension were spun through 33.8% Percoll (Sigma) for 12 min at 693*g*. Red blood cells in recovered cell pellets were removed with red blood cell lysis buffer (Sigma) before analysis. Lung cells were extracted after digestion of minced lungs for 1 h at 37 °C with DNAse I (50 U/ml), hyaluronidase (100 U/ml, Sigma) and liberase (0.28 U/ml; Roche). For microglia purification, brains were minced into fine pieces and incubated for 90 min at 37 °C with 100 μg/ml collagenase D. For microglia purification, brains were minced into fine pieces and incubated for 90 min at 37 °C with 100 μg/ml collagenase D. Cells were dissociated into single-cell suspensions by a combination of pipetting and vortexing and were then spun through 50% percoll (Sigma) for 45 min at 200*g*. Microglia were identified as $CD11b^{+}CD45^{int}$ by flow cytometry. In some experiments, microglia were further enriched to a purity of over 95% with CD11b magnetic beads (Miltenyi Biotech) and were stimulated with various TLR ligands (Invivogen) *in vitro* at the appropriate concentration. DCs from spleens and lymph nodes were dissociated into single-cell suspensions by incubation for 60 min with 100 μg/ml collagenase D before red blood cell lysis. In some experiment, DCs were further purified with CD11c magnetic beads (Miltenyi).

Viral infection

Wild-type WNV and WNV strain E218A were generated from an infectious cDNA clone of the New York 1999 strain and were propagated in C6/36 *Aedes albopictus* or BHK21-15 baby hamster kidney cells as described[56,57]. Vero African green monkey cells were used for measurement of viral titers of infected tissues by focus-forming assay[58]. Sex- and age-matched wild-type and *Il34*$^{LacZ/LacZ}$ mice 8–10 weeks of age were inoculated by intracranial injection with specified doses of WNV diluted in Hank's balanced-salt solution supplemented with 1% heat-inactivated FBS (1×10^5 PFU in 10 μl). On specific days after infection, mice were killed and extensively perfused with iced PBS; organs were collected, weighed and processed for analysis of infiltrating CNS lymphocytes by a published protocol[53] or were stored at −80 °C until further processing. Alternatively, survival of groups of mice was monitored for 21 d after infection.

Ear painting, analysis of CHS and delayed-type hypersensitivity and treatment with ultraviolet light

The migration of DCs and LCs was asssessed by painting of mouse ears with 100 μl 0.5% CellTracker Green (invitrogen) in acetone and dibutylphthalate (1:1) at 40–48 h before collection of cervical lymph nodes. CHS was induced in mice as described[59]. Mice were sensitized on day 0 by topical application, on the shaved abdomen, of 25 μl of 0.5% DNFB (2,4 dinitroflurobenzene; Sigma) in a mixture of acetone and olive oil (4:1). On day 5, mice were challenged with 10 μl of 0.2% DNFB on the left ear and 10 μl of vehicle on the right ear. Ear swelling was measured with an engineer's micrometer (Fowler) 24 h after challenge. T cell priming during CHS was assessed as described[60]. Mice were sensitized by two daily paintings (days 0 and 1), on the shaved abdomen, of 25 μl of 0.5% DNFB. Inguinal lymph node cells from sensitized and control mice were cultured for 2 d in the presence of plate bound anti-CD3 (1 μg/ml; eBio500A2; eBioscience). IFN-γ in the supernatant was measured by cytometric bead array with a mouse inflammation kit (BD Bioscience). Induction of delayed-type hypersensitivity by *C. albicans* has been described[61]. Mice were shaved and chemically depilated with Nair hair remover. The stratum corneum was removed with 15 strokes with 220-grit sandpaper (3M). *C. albicans* was grown at 30 °C in yeast-peptone-adenine-dextrose medium until the absorbance at 600 nm reached 1.5–2.0. *C. albicans* (2×10^8 in 50 μl sterile PBS) was applied on to the skin. At 8 d after skin infection, mice were challenged with footpad injection of 1×10^7 heat-killed *C. albicans*. The specific delayed-type hypersensitivity was determined on the basis of the degree of footpad swelling 24 h after challenge. Treatment with ultraviolet light was done as described[16].

Flow cytometry

DCs and other cell types in single-cell suspensions were incubated with supernatant of the hybridoma HB-197 (American Type Culture COllection) for blockade of Fc receptors and stained with anti-CD3 (145-2c11), anti-CD4 (GK1.5), anti-CD8α (53–6.7), anti-CD44 (IM7), anti-Ly6C (AL-21), anti-MHC-II (I-A/I-E, 2G9 or M5/114.15.2), anti-Siglec-F (E50-2440), anti-CD11b (M1/70; all from BD Pharmingen); anti-Ly6G (1A8), anti-CD62L (MEL-14), anti-Siglec-H (551; all from Biolegend); anti-CD11c (N418), anti-CD45 (30-F11), anti-CD103 (2E7; all from eBioscience); and anti body to the H-2D^b–NS4B tetramer (US National Institutes of Health tetramer core facility). For intracellular staining with anti-CD207 (L31; eBioscience) and anti–granzyme B (GB12; Invitrogen), surfaces of cells were stained, then cells were fixed and permeabilized with Cytofix/Cytoperm buffer (BD Bioscience). Cells were processed on a FACSCalibur or FACSCanto II (BD Bioscience) and analyzed with FlowJo software (Tree Star).

Statistics

GraphPad Prism (GraphPad software) was used for all statistics analyses.

Supplementary Material

Refer to Web version on PubMed Central for supplementary material.

Acknowledgments

We thank M. Swiecki for help with flow cytometry and confocal microscopy; the European Conditional Mouse Mutagenesis Consortium for generating embryonic stem clones with the targeted allele *Il34*$^{tm1a(EUCOMM)Wtsi}$; M. White for injection of *Il34*$^{tm1a(EUCOMM)Wtsi}$ embryonic stem cells; and T. Doering (Department of Molecular Microbiology, Washington University School of Medicine) for *C. albicans* SC5314. Supported by the National Heart, Lung and Blood Institute (2T32HL007317-31 to Y.W.), Fondazione Beretta (C.R.), Programma di Ricerca di interesse Nazionale of the Ministero dell'Istruzione dell'Università e della Ricerca, 2009 (W.V.), the European Commission Seventh Framework Programme (A.D.B.) and the US National Institutes of Health (GM77279 and HL097805 to M.Co.).

References

1. Gordon S, Mantovani A. Diversity and plasticity of mononuclear phagocytes. Eur J Immunol. 2011; 41:2470–2472. [PubMed: 21952798]
2. Geissmann F, et al. Development of monocytes, macrophages, and dendritic cells. Science. 2010; 327:656–661. [PubMed: 20133564]
3. Liu K, Nussenzweig MC. Origin and development of dendritic cells. Immunol Rev. 2010; 234:45–54. [PubMed: 20193011]
4. Merad M, Manz MG. Dendritic cell homeostasis. Blood. 2009; 113:3418–3427. [PubMed: 19176316]
5. Shortman K, Naik SH. Steady-state and inflammatory dendritic-cell development. Nat Rev Immunol. 2007; 7:19–30. [PubMed: 17170756]
6. Chitu V, Stanley ER. Colony-stimulating factor-1 in immunity and inflammation. Curr Opin Immunol. 2006; 18:39–48. [PubMed: 16337366]
7. Hamilton JA. Colony-stimulating factors in inflammation and autoimmunity. Nat Rev Immunol. 2008; 8:533–544. [PubMed: 18551128]
8. Teitelbaum SL, Ross FP. Genetic regulation of osteoclast development and function. Nat Rev Genet. 2003; 4:638–649. [PubMed: 12897775]
9. Choi JH, et al. Flt3 signaling-dependent dendritic cells protect against atherosclerosis. Immunity. 2011; 35:819–831. [PubMed: 22078798]
10. Cecchini MG, et al. Role of colony stimulating factor-1 in the establishment and regulation of tissue macrophages during postnatal development of the mouse. Development. 1994; 120:1357–1372. [PubMed: 8050349]
11. Yoshida H, et al. The murine mutation osteopetrosis is in the coding region of the macrophage colony stimulating factor gene. Nature. 1990; 345:442–444. [PubMed: 2188141]
12. Dai XM, et al. Targeted disruption of the mouse colony-stimulating factor 1 receptor gene results in osteopetrosis, mononuclear phagocyte deficiency, increased primitive progenitor cell frequencies, and reproductive defects. Blood. 2002; 99:111–120. [PubMed: 11756160]
13. Ransohoff RM, Cardona AE. The myeloid cells of the central nervous system parenchyma. Nature. 2010; 468:253–262. [PubMed: 21068834]
14. Witmer-Pack MD, et al. Identification of macrophages and dendritic cells in the osteopetrotic (op/op) mouse. J Cell Sci. 1993; 104:1021–1029. [PubMed: 8314887]
15. Ginhoux F, et al. Fate mapping analysis reveals that adult microglia derive from primitive macrophages. Science. 2010; 330:841–845. [PubMed: 20966214]
16. Ginhoux F, et al. Langerhans cells arise from monocytes *in vivo*. Nat Immunol. 2006; 7:265–273. [PubMed: 16444257]

17. Lin H, et al. Discovery of a cytokine and its receptor by functional screening of the extracellular proteome. Science. 2008; 320:807–811. [PubMed: 18467591]
18. Ma X, et al. Structural basis for the dual recognition of helical cytokines IL-34 and CSF-1 by CSF-1R. Structure. 2012; 20:676–687. [PubMed: 22483114]
19. Wei S, et al. Functional overlap but differential expression of CSF-1 and IL-34 in their CSF-1 receptor-mediated regulation of myeloid cells. J Leukoc Biol. 2010; 88:495–505. [PubMed: 20504948]
20. Chihara T, et al. IL-34 and M-CSF share the receptor Fms but are not identical in biological activity and signal activation. Cell Death Differ. 2010; 17:1917–1927. [PubMed: 20489731]
21. Chorro L, et al. Langerhans cell (LC) proliferation mediates neonatal development, homeostasis, and inflammation-associated expansion of the epidermal LC network. J Exp Med. 2009; 206:3089–3100. [PubMed: 19995948]
22. Merad M, Ginhoux F, Collin M. Origin, homeostasis and function of Langerhans cells and other langerin-expressing dendritic cells. Nat Rev Immunol. 2008; 8:935–947. [PubMed: 19029989]
23. Ginhoux F, Merad M. Ontogeny and homeostasis of Langerhans cells. Immunol Cell Biol. 2010; 88:387–392. [PubMed: 20309014]
24. Valladeau J, et al. Identification of mouse langerin/CD207 in Langerhans cells and some dendritic cells of lymphoid tissues. J Immunol. 2002; 168:782–792. [PubMed: 11777972]
25. Takahara K, et al. Identification and expression of mouse Langerin (CD207) in dendritic cells. Int Immunol. 2002; 14:433–444. [PubMed: 11978773]
26. Poulin LF, et al. The dermis contains langerin^{+} dendritic cells that develop and function independently of epidermal Langerhans cells. J Exp Med. 2007; 204:3119–3131. [PubMed: 18086861]
27. Ginhoux F, et al. Blood-derived dermal langerin^{+} dendritic cells survey the skin in the steady state. J Exp Med. 2007; 204:3133–3146. [PubMed: 18086862]
28. Bursch LS, et al. Identification of a novel population of Langerin^{+} dendritic cells. J Exp Med. 2007; 204:3147–3156. [PubMed: 18086865]
29. Romani N, Clausen BE, Stoitzner P. Langerhans cells and more: langerin-expressing dendritic cell subsets in the skin. Immunol Rev. 2010; 234:120–141. [PubMed: 20193016]
30. Bennett CL, Noordegraaf M, Martina CA, Clausen BE. Langerhans cells are required for efficient presentation of topically applied hapten to T cells. J Immunol. 2007; 179:6830–6835. [PubMed: 17982073]
31. Bennett CL, et al. Inducible ablation of mouse Langerhans cells diminishes but fails to abrogate contact hypersensitivity. J Cell Biol. 2005; 169:569–576. [PubMed: 15897263]
32. Bacci S, Alard P, Dai R, Nakamura T, Streilein JW. High and low doses of haptens dictate whether dermal or epidermal antigen-presenting cells promote contact hypersensitivity. Eur J Immunol. 1997; 27:442–448. [PubMed: 9045915]
33. Enk AH, Katz SI. Early events in the induction phase of contact sensitivity. J Invest Dermatol. 1992; 99:39S–41S. [PubMed: 1385542]
34. Kissenpfennig A, et al. Dynamics and function of Langerhans cells in vivo: dermal dendritic cells colonize lymph node areas distinct from slower migrating Langerhans cells. Immunity. 2005; 22:643–654. [PubMed: 15894281]
35. Ruedl C, Koebel P, Bachmann M, Hess M, Karjalainen K. Anatomical origin of dendritic cells determines their life span in peripheral lymph nodes. J Immunol. 2000; 165:4910–4916. [PubMed: 11046016]
36. Christensen AD, Haase C. Immunological mechanisms of contact hypersensitivity in mice. APMIS. 2012; 120:1–27. [PubMed: 22151305]
37. Igyártó BZ, et al. Skin-resident murine dendritic cell subsets promote distinct and opposing antigen-specific T helper cell responses. Immunity. 2011; 35:260–272. [PubMed: 21782478]
38. Getts DR, et al. Ly6c^{+} “inflammatory monocytes” are microglial precursors recruited in a pathogenic manner in West Nile virus encephalitis. J Exp Med. 2008; 205:2319–2337. [PubMed: 18779347]

39. Crispe IN. The liver as a lymphoid organ. Annu Rev Immunol. 2009; 27:147–163. [PubMed: 19302037]
40. Kinoshita M, et al. Characterization of two F4/80-positive Kupffer cell subsets by their function and phenotype in mice. J Hepatol. 2010; 53:903–910. [PubMed: 20739085]
41. Merad M, et al. Langerhans cells renew in the skin throughout life under steady-state conditions. Nat Immunol. 2002; 3:1135–1141. [PubMed: 12415265]
42. Takahashi K, Naito M, Shultz LD. Differentiation of epidermal Langerhans cells in macrophage colony-stimulating-factor-deficient mice homozygous for the osteopetrosis (op) mutation. J Invest Dermatol. 1992; 99:46S–47S. [PubMed: 1431208]
43. Anandasabapathy N, et al. Flt3L controls the development of radiosensitive dendritic cells in the meninges and choroid plexus of the steady-state mouse brain. J Exp Med. 2011; 208:1695–1705. [PubMed: 21788405]
44. Ajami B, Bennett JL, Krieger C, McNagny KM, Rossi FM. Infiltrating monocytes trigger EAE progression, but do not contribute to the resident microglia pool. Nat Neurosci. 2011; 14:1142–1149. [PubMed: 21804537]
45. Jiang A, et al. Disruption of E-cadherin-mediated adhesion induces a functionally distinct pathway of dendritic cell maturation. Immunity. 2007; 27:610–624. [PubMed: 17936032]
46. Romani N, Brunner PM, Stingl G. Changing views of the role of langerhans cells. J Invest Dermatol. 2012; 132:872–881. [PubMed: 22217741]
47. Kaplan DH, Jenison MC, Saeland S, Shlomchik WD, Shlomchik MJ. Epidermal langerhans cell-deficient mice develop enhanced contact hypersensitivity. Immunity. 2005; 23:611–620. [PubMed: 16356859]
48. Kaplan DH. In vivo function of Langerhans cells and dermal dendritic cells. Trends Immunol. 2010; 31:446–451. [PubMed: 21035396]
49. Prinz M, Priller J, Sisodia SS, Ransohoff RM. Heterogeneity of CNS myeloid cells and their roles in neurodegeneration. Nat Neurosci. 2011; 14:1227–1235. [PubMed: 21952260]
50. Paolicelli RC, et al. Synaptic pruning by microglia is necessary for normal brain development. Science. 2011; 333:1456–1458. [PubMed: 21778362]
51. Schwenk F, Baron U, Rajewsky K. A cre-transgenic mouse strain for the ubiquitous deletion of loxP-flanked gene segments including deletion in germ cells. Nucleic Acids Res. 1995; 23:5080–5081. [PubMed: 8559668]
52. Kanki H, Suzuki H, Itohara S. High-efficiency CAG-FLPe deleter mice in C57BL/6J background. Exp Anim. 2006; 55:137–141. [PubMed: 16651697]
53. Szretter KJ, et al. The immune adaptor molecule SARM modulates tumor necrosis factor α production and microglia activation in the brainstem and restricts West Nile Virus pathogenesis. J Virol. 2009; 83:9329–9338. [PubMed: 19587044]
54. Samuel MA, Morrey JD, Diamond MS. Caspase 3-dependent cell death of neurons contributes to the pathogenesis of West Nile virus encephalitis. J Virol. 2007; 81:2614–2623. [PubMed: 17192305]
55. Kinoshita M, et al. Characterization of two F4/80-positive Kupffer cell subsets by their function and phenotype in mice. J Hepatol. 2010; 53:903–910. [PubMed: 20739085]
56. Daffis S, et al. 2′-O methylation of the viral mRNA cap evades host restriction by IFIT family members. Nature. 2010; 468:452–456. [PubMed: 21085181]
57. Vogt MR, et al. Human monoclonal antibodies against West Nile virus induced by natural infection neutralize at a postattachment step. J Virol. 2009; 83:6494–6507. [PubMed: 19386704]
58. Fuchs A, Pinto AK, Schwaeble WJ, Diamond MS. The lectin pathway of complement activation contributes to protection from West Nile virus infection. Virology. 2011; 412:101–109. [PubMed: 21269656]
59. Girardi M, et al. Resident skin-specific gammadelta T cells provide local, nonredundant regulation of cutaneous inflammation. J Exp Med. 2002; 195:855–867. [PubMed: 11927630]
60. Xu H, DiIulio NA, Fairchild RL. T cell populations primed by hapten sensitization in contact sensitivity are distinguished by polarized patterns of cytokine production: interferon gamma-producing (Tc1) effector $CD8^+$ T cells and interleukin (Il) 4/Il-10-producing (Th2) negative regulatory $CD4^+$ T cells. J Exp Med. 1996; 183:1001–1012. [PubMed: 8642241]

61. Igyártó BZ, et al. Skin-resident murine dendritic cell subsets promote distinct and opposing antigen-specific T helper cell responses. Immunity. 2011; 35:260–272. [PubMed: 21782478]

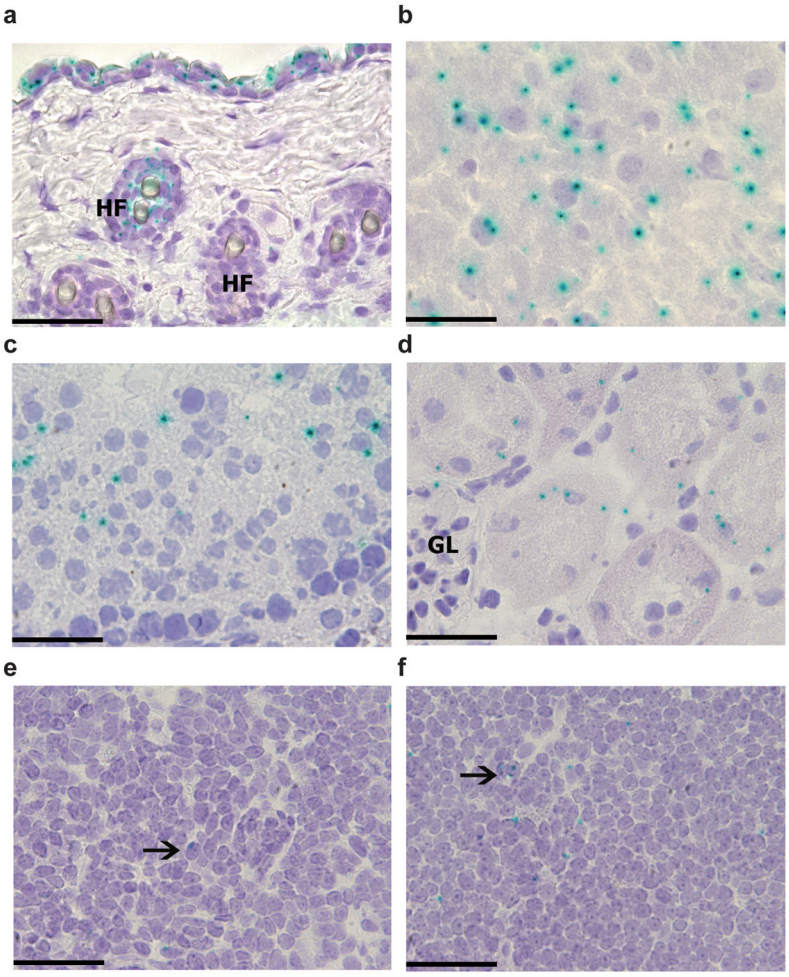

Figure 1.

Tissue specific expression of IL-34. Staining for X-gal (blue) in skin (**a**), brain cerebral cortex (**b**), testis (**c**), kidney tubules (**d**), spleen (**e**) and lymph nodes (**f**) from *Il34*$^{LacZ/LacZ}$ mice. Tissues from wild-type mice did not show any X-gal staining (data not shown). HF, hair follicles; GL, kidney glomerulus. Arrows indicate X-gal^{+} cells. Original magnification, ×400 (**a**; scale bar, 50 μm) or ×600 (**b**–**f**; scale bars, 33 μm). Data are representative of 2 experiments with three mice (25 high-power fields per tissue per mouse).

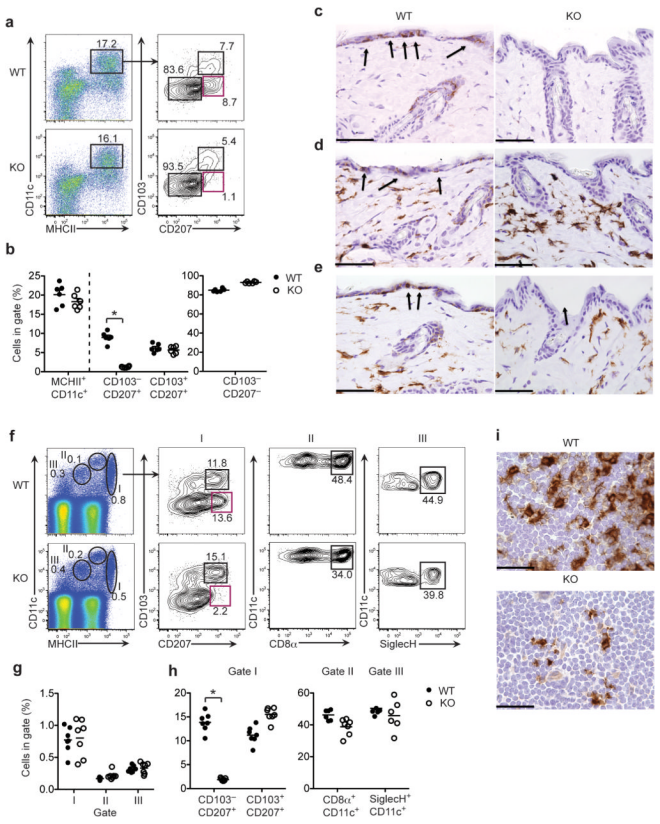

Figure 2.

IL-34 deficiency leads to the absence of LCs. (**a**, **b**) Flow cytometry of single-cell suspensions of wild-type (WT) and *Il34*$^{LacZ/LacZ}$ (KO) skin digests stained for CD45, CD11c, MHCII, CD103 and intracellular CD207 (langerin). (**a**) Gating of CD11c^{+}MHCII^{+} cells among live CD45^{+} cells (left), followed by further discrimination (right) of LCs (CD103^{-}CD207^{+}) and dermal DCs (CD103^{+}CD207^{+} and CD103^{-}CD207^{-}). (**b**) Frequency of total CD11c^{+}MHCII^{+} cells (among live CD45^{+} cells), LCs and dermal DCs (among CD11c^{+}MHCII^{+} cells) in the skin of wild-type and *Il34*$^{LacZ/LacZ}$ mice (n = 6 per group). *P < 0.0001, (unpaired Student's t-test). (**c**–**e**) Immunohistochemical analysis of langerin (brown; **c**), MHCII (brown; **d**) and CD11b (brown; **e**) in the skin of wild-type and *Il34*$^{LacZ/LacZ}$ mice. Arrows indicate positive cells in the epidermis. Original magnification, ×400 (scale bars, 50 μm). (**f**) Flow cytometry of single-cell suspensions of wild-type and *Il34*$^{LacZ/LacZ}$ skin-draining lymph nodes stained for CD11c and MHCII to identify DC subsets (left), followed by further analysis (right) of CD11c^{+}MHCII^{hi} cells (I) to determine the frequency of migrating LCs and CD103^{+} dermal DCs; of CD11c^{hi}MCHII^{int} cells (II) to determine the frequency of CD8α^{+} DCs; and of CD11c^{lo}MHCII^{lo} cells (III) to determine the frequency of pDCs marked by expression of Siglec-H. (**g**) Frequency of CD11c^{+}MCHII^{+} cells in gates I, II, and III. (**h**) Frequency of CD103^{-}CD207^{+} LCs, CD103^{+}CD207^{+} dermal DCs (in gate I), CD8α^{+} DCs (in gate II) and pDCs (in gate III) in the skin-draining lymph nodes of wild-type and *Il34*$^{LacZ/LacZ}$ mice (n = 6 or 7 per group). (**i**) Immunohistochemistry analysis of langerinin cervical lymph nodes of wild-type and *Il34*$^{LacZ/LacZ}$ mice. Original magnification, ×600 (scale bars, 33 μm). Numbers adjacent to outlined areas (**a**, **f**) indicate percent cells in each gate. Each symbol (**b**, **g**, **h**) represents an individual mouse; small horizontal lines indicate the mean. *P < 0.0001 (unpaired Student's t-test). Data represent at least two independent experiments.

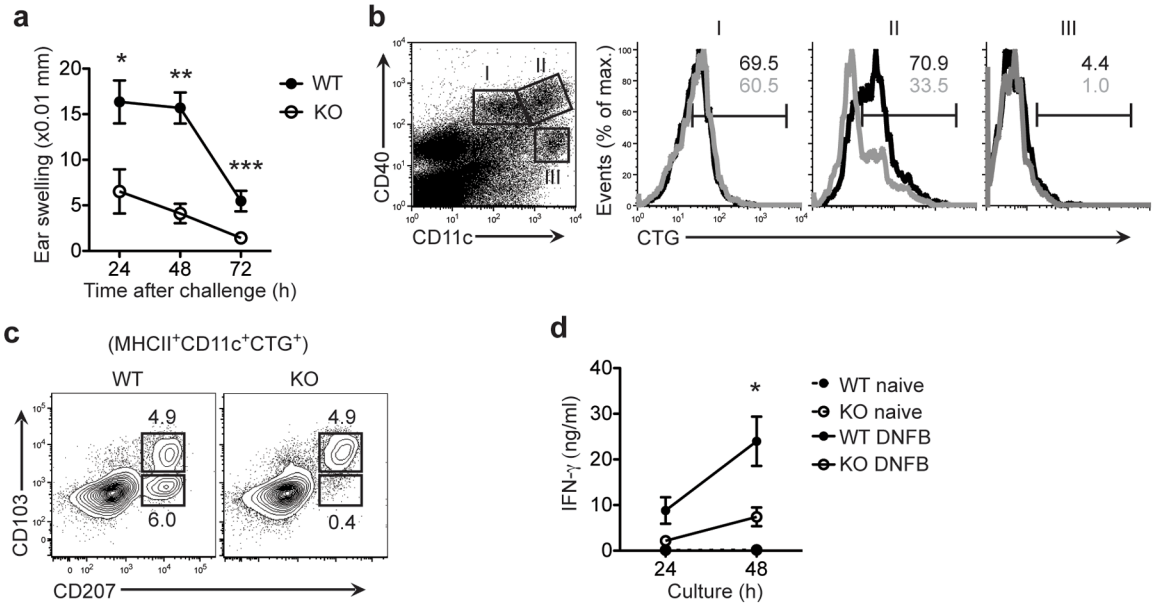

Figure 3.

IL-34 deficiency leads to diminished DNFB-mediated CHS. (**a**) Ear swelling in wild-type mice ($n = 6$) and *Il34*$^{LacZ/LacZ}$ mice ($n = 7$) at 24, 48 and 72 h after challenge with DNFB. *$P = 0.015$, **$P < 0.0001$ and ***$P = 0.0034$ (unpaired Student's *t*-test). (**b**) Flow cytometry of cells from the ear-draining lymph nodes of wild-type and *Il34*$^{LacZ/LacZ}$ mice after painting of ears with CellTracker green. Left panel, DCs were separated as CD11c^{int}CD40^{int} cells (population I), CD11c^{hi}CD40^{hi} cells (population II) and CD11c^{hi}CD40^{lo} cells (population III). Right, flow cytometry of cells in the populations gated at left (black lines, wild-type; gray lines, *Il34*$^{LacZ/LacZ}$). Numbers above bracketed lines (colors match line colors) indicate percent cells positive for CellTracker green (CTG). (**c**) Flow cytometry of MHCII^{hi}CD11c^{+}CTG^{+} cells at 48 h after the ear painting in **b**, to assess the migration of LCs and dermal DCs. Numbers adjacent to outlined areas indicate percent CD103^{+}CD207^{+} cells (bottom) or CD103^{+}CD207^{+} cells (top). (**d**) IFN-γ in skin-draining (inguinal) lymph nodes isolated from wild-type and *Il34*$^{LacZ/LacZ}$ mice without sensitization (naive) or 6 d after DNFB sensitization (DNFB). Lymph node cells (2×10^5 cells/well) were cultured for 24 or 48 h in the presence of plate-bound anti-CD3 and cytometric bead array analysis of culture supernatants. *$P = 0.04$ (unpaired Student's *t*-test). Data are representative of three independent experiments (**a**), represent two independent experiments with two mice per group (**b**, **c**) or represent one of two independent experiments with three mice per group in each (**d**).

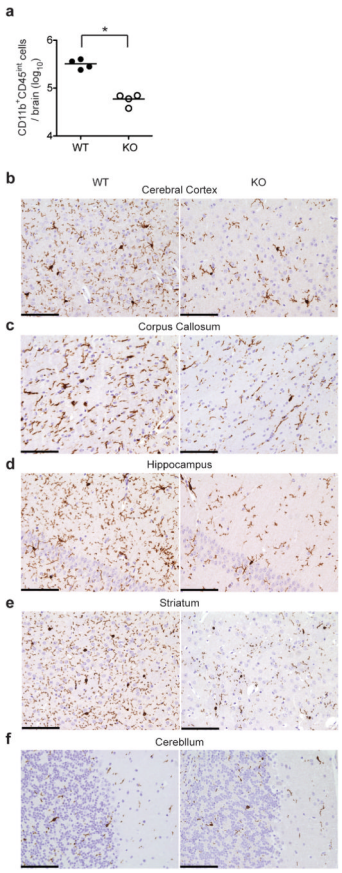

Figure 4.

Impaired microglia development in IL-34-deficient mice. (**a**) Total $CD45^{int}CD11b^{+}$ microglial cells in the brains of wild-type and *Il34*$^{LacZ/LacZ}$ mice (n = 4 per group). Each symbol represents an individual mouse; small horizontal lines indicate the mean. *P = 0.0004 (unpaired Student's t-test). (**b**–**f**) Immunohistochemistry of wild-type and *Il34*$^{LacZ/LacZ}$ mouse cerebral cortex (**b**), corpus callosum (**c**), hippocampus (**d**), striatum (**e**) and cerebellum (**f**) in fixed brain tissues stained with the myeloid marker IBA-1. Original magnification, ×200 (scale bars, 100 μm). Data are representative of three experiments (**a**) or represent two independent experiments (**b**–**f**).

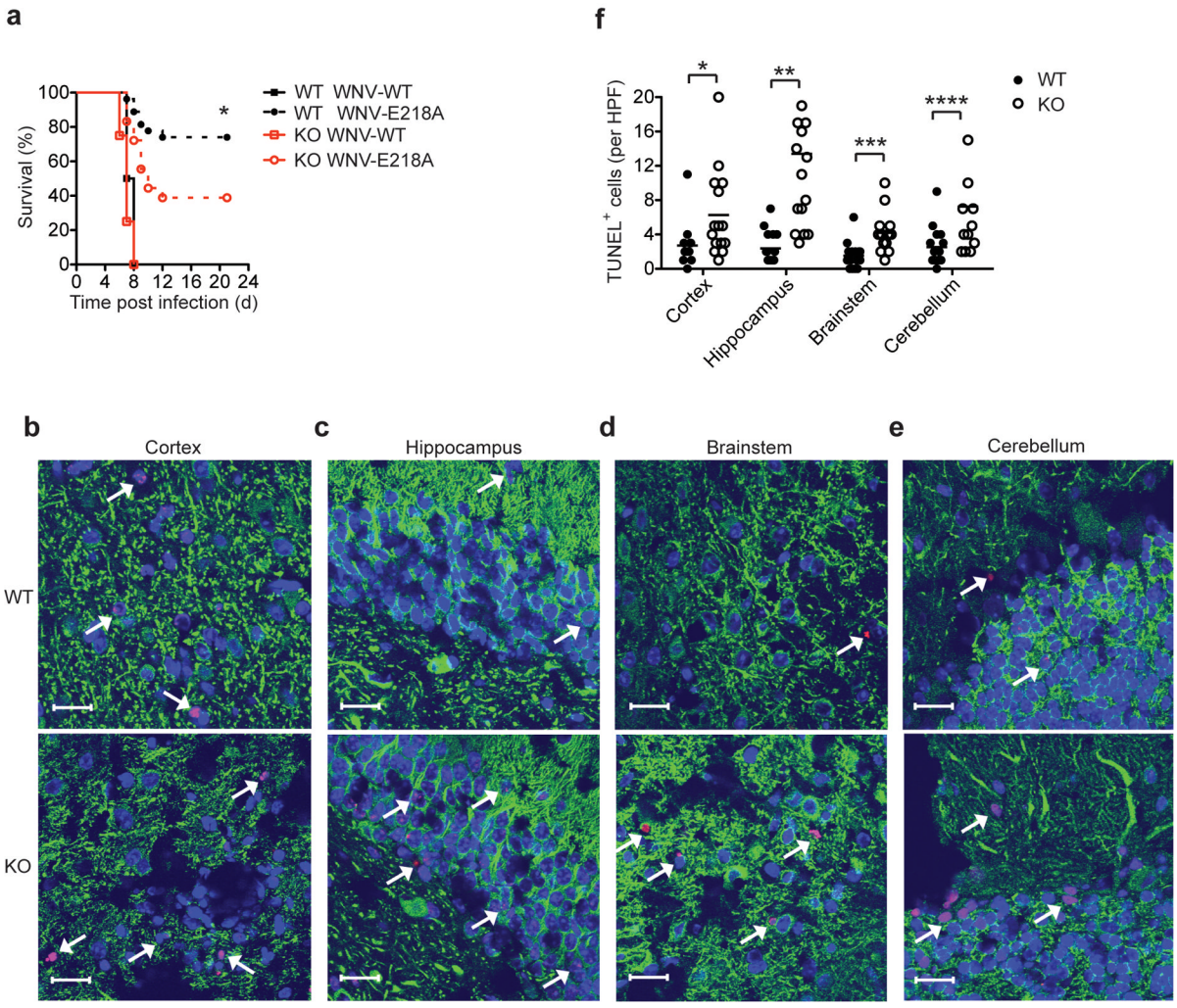

Figure 5.

IL-34-deficient mice are more susceptible to infection after intracranial inoculation of attenuated WNV. (**a**) Survival of 9-week-old wild-type mice (*n = 27*) and *Il34*$^{LacZ/LacZ}$ mice (*n = 18*) inoculated via an intracranial route with wild-type WNV (10 plaque-forming units) or attenuated WNV (WNV-E218A; 1 × 10^5 plaque-forming units) and monitored for 21 d. **P* = 0.0155 (Gehan-Breslow-Wilcoxon test). (**b**–**e**) Microscopy of fixed, frozen sections of the cerebral cortex (**b**), hippocampus (**c**), brainstem (**d**) and cerebellum (**e**) of wild-type and *Il34*$^{LacZ/LacZ}$ mice infected by intracranial injection of attenuated WNV (1 × 10^5 PFU), assessed at day 6 after infection by staining for the neuronal antigen MAP-2 (green), TUNEL analysis (red) and nuclear staining with ToPro-3 (blue). Arrows indicate TUNEL$^+$ neurons. Original magnification, ×63 (scale bars, 20 μm). (**f**) Quantification of TUNEL$^+$ cells in **b**–**e** (*n* = 4 mice; three high-power fields (HPF) per brain region per mouse). Each symbol represents an individual mouse; small horizontal lines indicate the mean. **P* = 0.0268, ***P* < 0.0001, ****P* = 0.0005 and **** *P* = 0.0077 (unpaired Student's *t*-test). Data represent three independent experiments (**a**) or one experiment with four to six mice per group (**b**–**f**).

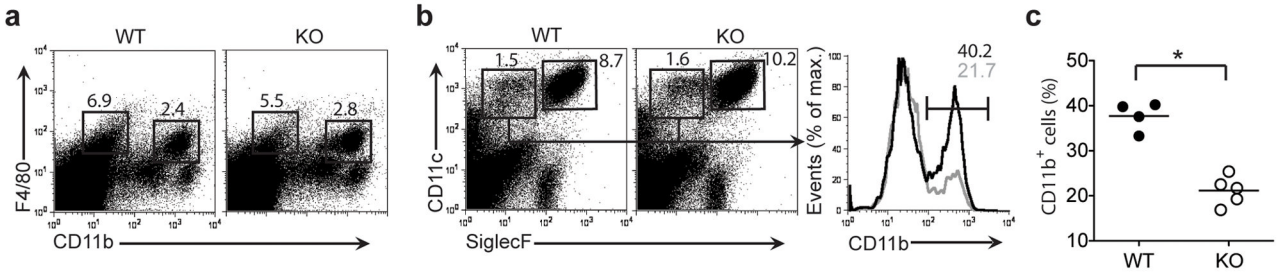

Figure 6.

IL-34 deficiency does not affect the development of myeloid cells in the liver but partially affects the frequency of CD11b$^+$ DCs in the lungs. (**a**) Flow cytometry of single-cell suspensions of wild-type and *Il34*$^{LacZ/LacZ}$ liver cells, to identify two subsets of Kupffer cells. Numbers above outlined areas indicate percent F4/80$^+$CD11b$^-$ cells (left) and F4/80$^+$CD11b$^+$ cells (right). (**b**) Flow cytometry of cells from the lungs of wild-type and *Il34*$^{LacZ/LacZ}$ mice (left). Numbers adjacent to outlined areas indicate percent CD11c$^+$Siglec-F$^+$ cells (lung alveolar macrophages; right) and CD11c$^+$Siglec-F$^-$ cells (lung DCs; left). Right, frequency (numbers above brackets) of CD11b$^+$ lung DCs in wild-type mice (black lines) and *Il34*$^{LacZ/LacZ}$ mice (gray lines). (**c**) Frequency of CD11b$^+$ DCs among CD11c$^+$Siglec-F$^-$ DCs in wild-type and *Il34*$^{LacZ/LacZ}$ mouse lungd. Each symbol represents an individual mouse; small horizontal lines indicate the mean. **P* = 0.0001 (unpaired Student's *t*-test). Data represent two independent experiments with at least two mice per group.

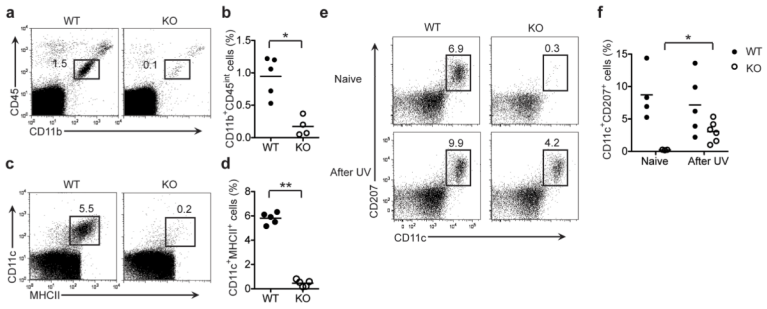

Figure 7.

IL-34 is required for the development of microglia and LCs in neonates but is dispensable for recolonization of LCs in adult mice after exposure to ultraviolet light. (**a–d**) Flow cytometry of cells from the brain (**a**, **b**) and epidermis (**c**, **d**) of neonatal (2-day-old) wild-type and *Il34*$^{LacZ/LacZ}$ mice (n = 5–6 per group). Numbers adjacent to outlined areas (**a**, **c**) indicate percent CD45^{int}CD11b^{+} cells (microglia; **a**) or CD11c^{+}MHCII^{+} cells (LCs; **c**). (**b**, **d**) Frequency of microglia (CD45^{int}CD11b^{+}; **b**) and LCs (CD11c^{+}CD207^{+}; **d**) in the CD45^{+} gate. *P = 0.0025 and **P < 0.0001 (unpaired Student's t-test). (**e**, **f**) Flow cytometry of cells from wild-type and *Il34*$^{LacZ/LacZ}$ mice (n = 3–6 per group) left untreated (Naive) or irradiated with ultraviolet light (UV; assessed on day 21). Numbers above outlined areas indicate percent CD207^{+}CD11c^{+} cells. (**f**) Quantification of the analysis in **e**. *P = 0.0083 (unpaired Student's t-test). Each symbol (**b**, **d**, **f**) represents an individual mouse; small horizontal lines indicate the mean. Data represent two independent experiments.

Table 1

Numbers of microglial cells in various regions of the brains of wild-type and *Il34*$^{LacZ/LacZ}$ mice

Region	Cell count		*P*
	WT	KO	
Cerebral cortex	10.3 (2.6)	3.7 (1.8)	<0.0001
Corpus callosum	5.6 (1.8)	2.8 (1.5)	<0.001
Hippocampus	7.3 (2.9)	3.0 (1.7)	<0.001
Striatum	7.4 (2.4)	4.2 (2.2)	<0.01
Cerebellum	3.5 (1.5)	2.9 (1.3)	0.055

Quantification of microglial cells in wild-type and *Il34*$^{LacZ/LacZ}$ mice cell, assessed by microscopy (×400) of paired regions of the brain stained with anti-IBA-1. Data are representative of one experiment with at least 25 high-power fields per region per mouse (mean and s.d.; 3 mice/group).